Mem. S.A.It. Vol. 78, 98

Memorie della

Dual-line analysis of sunspot oscillations

K. Tziotziou[1], G. Tsiropoula[1], N. Mein[2], and P. Mein[2]

[1] National Observatory of Athens, Institute for Space Applications and Remote Sensing, Lofos Koufos, 15236 Palea Penteli, Greece
e-mail: kostas@space.noa.gr
[2] Observatoire de Paris, Section de Meudon, LESIA, F-92195 Meudon Principal Cedex, France

Abstract. Umbral oscillations and running penumbral (RP) waves are studied with simultaneous, two-dimensional, high cadence (8 sec), dual-line sunspot observations in Ca II 8542 Å and Hα, obtained with the MSDP spectrograph on the German VTT in Tenerife. Doppler velocity and intensity images are used to investigate the physical characteristics of umbral flashes (UFs) and RP waves while a wavelet spectral and phase analysis shows their temporal behaviour and permits us to elaborate on their nature and possible association.

Key words. Sun: chromosphere – Sun: oscillations – Sun: sunspots

1. Introduction

Sunspots exhibit a wide range of oscillatory phenomena within their umbrae and penumbrae. Their study started with the detection of umbral flashes (UFs) in Ca H and K intensity images and the infrared triplet of Ca by Beckers & Tallant (1969), while intensity and velocity observations in various spectral lines showed the existence of umbral photospheric oscillations (Bhatnagar et al., 1972), chromospheric oscillations (Beckers & Schultz, 1972; Giovanelli, 1972) and of running penumbral (RP) waves (Zirin & Stein, 1972; Giovanelli, 1972).

Umbral oscillations show dominant periods within the 5-min band at the photospheric level with an average rms velocity amplitude of 75 $\mathrm{m\,s^{-1}}$ (Lites, 1992) and the 3-min band at the chromospheric level (Brynildsen et al., 1999) with typical velocity amplitudes of ∼6-8 $\mathrm{km\,s^{-1}}$ (Tsiropoula et al., 2000). The umbra does not oscillate as a whole but oscillations rather occur in small spatial regions (oscillating elements) with sizes of 3″–4″ (Lites, 1986; Christopoulou et al., 2003). UFs appear as transient brightenings in parts of the umbra at chromospheric heights with periods of 2-3 min. UFs and umbral oscillations are probably different manifestations of the same phenomenon since the former occur only locally and occasionally when the velocity amplitudes exceed a value while the latter are always present in almost every sunspot umbra.

RP waves are seen as disturbances propagating radially from the umbra-penumbra boundary out to the edge of the penumbra and becoming gradually invisible, with a characteristic pattern – mainly in velocity images – of alternating dark and bright arcs with radial extents of 2300 – 3800 km and azimuthal extents of 90°– 180° and sometimes even 360° (see review by Bogdan & Judge, 2006). Their prop-

Send offprint requests to: K. Tziotziou

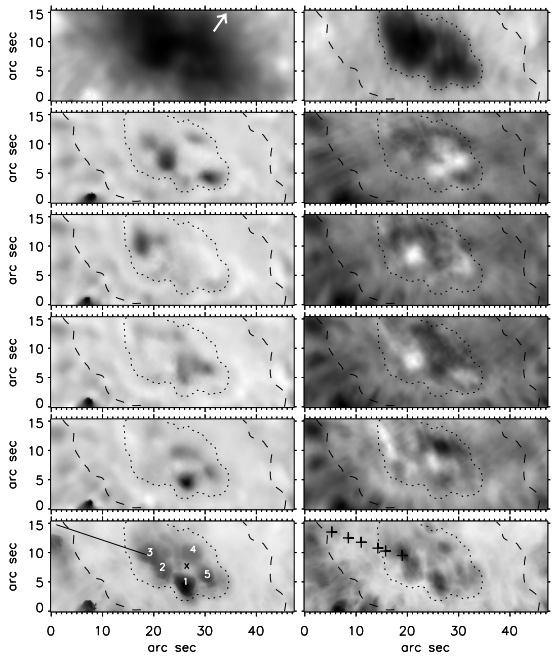

Fig. 1. *Top row*: A Ca II 8542 Å intensity image at ±0.135 Å (*left*) and the corresponding Hα one at ±0.58 Å (*right*) of the sunspot. North is towards the top, West towards the left of the panels, while the white arrow shows the direction to solar disc center. *Second to fifth row*: A sequence of Doppler velocity images in Ca II 8542 Å at ±0.135 Å (*left column*) and Hα at ±0.58 Å (*right column*). Time runs from top to bottom and the shown cadence is 32s. *Bottom row*: The distribution of the highest amplitude downward Doppler velocity per pixel over the whole sequence in Ca II 8542 Å at ±0.09 Å (*left panel*) and in Hα at ±0.29 Å (*right panel*). White numbers indicate the 5 distinct UF positions while "x" marks the calmest umbral position. The overplotted line indicates the cut used for the time slice image of Fig. 2 and "+" signs mark the positions of the Doppler velocity profiles of Fig. 3. In all Doppler velocity panels black denotes downward Doppler velocities, while dotted and dashed contours show respectively the approximate Hα umbra-penumbra and outer penumbra boundaries.

agation velocities and velocity amplitudes decrease from the inner to the outer edges of the penumbra (Tsiropoula et al., 2000), while their oscillation period has a dominant peak within the 5-min band (Tziotziou et al., 2002).

The association of RP waves to umbral oscillations and UFs is still unclear although it is widely accepted that they must be related. Alissandrakis et al. (1992), Tsiropoula et al. (1996, 2000) provide evidence of waves originating in oscillating umbral elements and propagating to the penumbra. Christopoulou et al. (2000) claim that RP waves are not the continuation of umbral oscillations into the penumbra, while Rouppe van der Voort et al. (2003), Bogdan & Judge (2006) suggest that UFs and RP waves share a common extended source below the visible photosphere and RP waves are not a physical wave but rather a visual pattern of upward propagating wavefronts along individual magnetic field lines of longer length and greater inclination with respect to the vertical.

The aim of this work is to further study umbral and penumbral oscillations and their association.

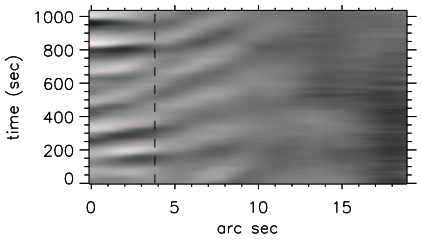

Fig. 2. Hα Doppler velocity at ±0.29 Å along the cut shown in Fig. 1 as a function of time. Black represents downward velocities, length runs from the umbra towards the edge of the penumbra and the vertical dashed line indicates the approximate umbra-penumbra boundary.

2. Observations

We are studying a sunspot (NOAA 9641, S13 W19) observed on October 4, 2001 with the German solar Vacuum Tower Telescope (VTT) in Tenerife, Canary Islands (see Fig. 1, *top row*). We used the Multichannel Subtractive Double Pass (MSDP) spectrograph (Mein, 1991, 2002) which is designed to record two-dimensional fields of view (FOV) at several wavelengths within a line profile. Observations of the same FOV were carried out simultaneously in the Hα and the infrared Ca II 8542 Å line from 09:53:39 to 10:10:51 UT, with a cadence of 8 s and a spatial resolution of $\sim$1″. After reduction and careful co-alignment, 130 183.5″× 19″ intensity and Doppler velocity images have been obtained for each line. Using the bisector technique, with the mean profile over the FOV as the reference profile, we have intensity and Doppler velocity images at ±0.29 Å and ±0.58 Å for Hα and at ±0.09 Å and ±0.135 Å for Ca II 8542 Å (positive Doppler shifts correspond to upward Doppler velocities and show up as bright in velocity images).

2.1. Umbral flashes and RP waves

UFs are visible in Hα as high upward or downward Doppler velocities within the umbra, while in Ca II 8542 Å they only show up as high downward Doppler velocities (Fig. 1, *second to fifth row*). The latter is a result of both the intricate nature of the Ca II 8542 Å UF profile which shows an emission on its blue side supposedly caused by the upward movement of hot material (Kneer et al., 1981; Uexküll et al., 1983; Tziotziou et al., 2002) and the derivation of Doppler velocities with the bisector method. UFs appear periodically at almost the same position in several distinct places within the umbra, either growing in amplitude and diffusing at the same position or diffusing by slow spreading in their vicinity. Their spatial distribution in both lines (Fig. 1, *bottom row*) is quite similar; at least five quite extended UFs are visible that fill almost the whole umbra.

3. Results

RP waves show up in Doppler velocity images (Fig. 1, *second to fifth row*) as propagating arcs in the penumbra, with an azimuthal extent – in our case – of at least 140° on its left (southwest) side, starting at the umbra-penumbra boundary. The time slice image of Fig. 2 shows a characteristic pattern of alternating downward and upward Doppler velocities which is concave upwards, indicating a decreasing propagation velocity as RP waves move outwards. Most of the waves can be traced back inside the umbra (seem to be a continuation of umbral waves) and their propagation looks smooth across the umbra–penumbra boundary.

3.1. Umbral and penumbral velocities

In Fig. 3 we present a series of Hα and Ca II 8542 Å Doppler velocity variations at certain positions presented in Fig. 1 as marked. The top row corresponds to Doppler velocity variations at an umbral flash position, second row at an umbral position just before the umbra-penumbra boundary, third and fourth rows at positions within the inner penumbra while the fifth and sixth rows show Doppler velocity variations in the outer penumbra. We can see that a) as we move from the umbra towards the edge of the penumbra the Doppler velocity amplitude decreases, while the period of the oscillations increases b) the downward (nega-

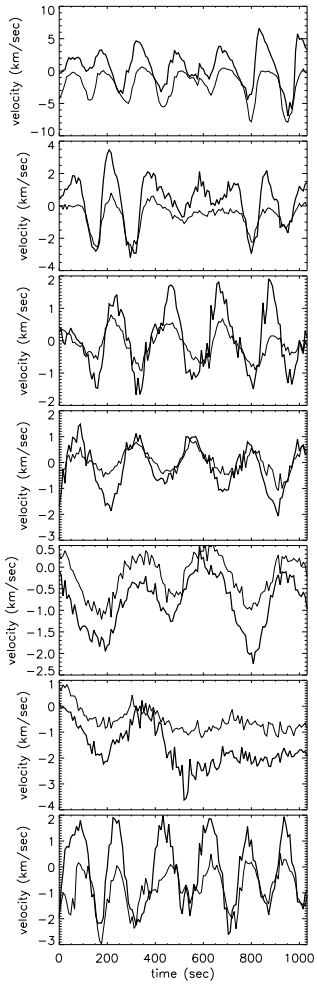

Fig. 3. *Top to sixth row*: A series of Hα Doppler velocity variations with time at ±0.29 Å (thick solid line) and the corresponding Ca II 8542 Å ones at ±0.09 Å (thin solid line) at positions marked with a "+" sign in Fig. 1. Doppler velocity variations run from top to bottom from the umbra outwards. *Bottom row*: Time evolution of the Doppler velocity for the calmest umbral position ("x" sign in Fig. 1). The thick solid line shows the Hα Doppler velocity at ±0.29 Å, the thin solid line the Ca II 8542 Å Doppler velocity at ±0.09 Å . Positive Doppler velocities represent upward motion.

tive) Ca II 8542 Å UF Doppler velocities are larger than the respective Hα ones while the upward (positive) UF Hα Doppler velocities are of the same order as the Hα downward ones and c) the Hα Doppler velocity curve has a clear sawtooth waveform, suggestive of a shock behavior of the corresponding oscillation. Furthermore, such a sawtooth behavior is seen also in the penumbra and probably as far as at the outer penumbra.

As Fig. 3 (*bottom panel*) shows, even the Hα Doppler velocity curve of the umbral position with the lowest amplitude velocities over time (calmest umbral position) shows a flash-like behavior, although much smoother than the UF one and with lower Doppler velocity amplitudes. This calmest umbral position is probably associated with velocity spreading from the neighboring UFs via running umbral waves.

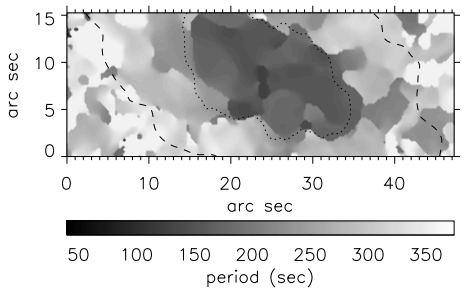

Fig. 4. Two-dimensional distribution of the dominant period at each pixel obtained with a wavelet analysis for the Ca II 8542 Å Doppler velocity variations at ±0.09 Å. The dotted and dashed black contours denote respectively the approximate Hα umbra-penumbra and outer penumbra boundaries.

3.2. Spectral and phase analysis

For the study of sunspot oscillations we are using a wavelet analysis (Torrence & Combo, 1998) while for finding the phase difference between two time series a cross-wavelet transform is performed (Tziotziou et al., 2005).

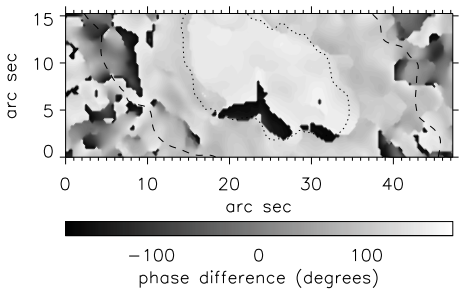

Fig. 5. Two-dimensional distribution of the global phase difference between the Ca II 8542 Å Doppler velocity and intensity variations at ±0.09 Å (the Doppler velocity curve is the reference curve). The dotted and dashed black contours denote respectively the approximate Hα umbra-penumbra and outer penumbra boundaries.

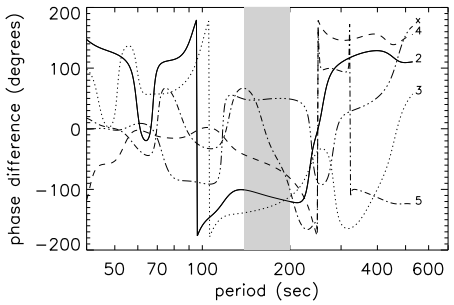

Fig. 6. Phase difference in Ca II 8542 Å obtained from Doppler velocity variations at ±0.135 Å for four UF positions and the calmest umbral position with the fifth UF velocity curve (No.1 in Fig. 1) used as a reference. The phase difference curves are marked with the corresponding numbers and signs shown in Fig. 1 and the shaded area shows the 3-min band which corresponds to the dominant oscillation period.

3.2.1. Periodicities

Fig. 4 shows the obtained two-dimensional distribution of the period corresponding to the maximum of the global power spectrum of the wavelet analysis for the Ca II 8542 Å Doppler velocity variations (the Hα distribution is qualitatively and quantitatively similar). We see that the whole umbra shows coherent oscillating elements of size 2.5 to 5″ and the umbra and the penumbra show oscillations around the 3-min and the 5-min band respectively. Both the umbra–penumbra and the penumbra–superpenumbra boundaries are distinguishable since there is a noticeable jump in the oscillation period. This abrupt change, which could also be due to a very rapid but smooth transition that is not observed because of our spatial resolution, probably indicates drastic changes of the local physical conditions and/or the magnetic field line inclination.

3.2.2. Velocity-intensity phase analysis

Fig. 5 shows the two-dimensional distribution of the global phase difference which corresponds to the power spectrum maximum between the Ca II 8542 Å Doppler velocity and intensity variations at ±0.09 Å at each pixel of the image, with the Doppler velocity curve taken as the reference curve. The dominant phase difference is positive in the umbra and the penumbra with highest values (more than 130°) within the umbra (the strong negative phase differences in the lower left part of the umbra are an artifact due to the wraparound effect). This positive phase difference indicates a delay in the reaction of intensity to the respective velocity variation in accordance with the existence of shock-shaped Doppler velocity profiles in the umbra and the penumbra, while the smaller phase differences in the penumbra could reflect an increase in the density which would lead to faster compression. There are two remarkable sharp decreases of the dominant phase difference at the umbra-penumbra boundary and close to the penumbra-superpenumbra boundary which may reflect drastic changes of the local physical (i.e. density and/or magnetic) conditions.

3.2.3. Phase difference between UFs

Fig. 6 shows the phase difference in Ca II 8542 Å obtained from Doppler velocity variations at ±0.135 Å of the four flash positions

and the calmest umbra position with the fifth flash velocity curve (No.1 in Fig. 1) used as a reference. The derived phase difference values around the 3-min band, which is the dominant period of oscillation, show that three out of five UFs and the calmest umbral point are not in phase. Only flashes No.2 and 3 seem to be almost in phase while flash No.1 appears after all other flashes. This behaviour could mean that the observed UFs either represent several pistons independently acting in the umbra or different reactions of parts of the umbra – due to local physical and/or magnetic field differences – to a single piston mechanism; however, it is impossible to conclude from these observations which of the two hypotheses is valid. Furthermore, the results show that the calmest umbral position is the only one with a positive phase difference (appears well after all flashes) suggesting that it probably experiences the effects of UFs after propagation (velocity spreading).

4. Conclusions

Umbral oscillations and RP waves have been studied with high cadence simultaneous Ca II 8542 Å and Hα observations. The analysis revealed several UFs that seem to fill the whole umbra. The Doppler velocity temporal variations indicate a shock behaviour for UFs, as well as for umbral and RP waves and a smooth and continuous propagation of the latter, with decreasing however propagation velocity, from the umbra towards the outer penumbra.

The spectral analysis indicates oscillating elements of size 2.5–5″ within the umbra with periods around the 3-min band and oscillation periods around the 5-min band in the penumbra. It also shows an increasing oscillatory period from the umbra outwards and two remarkable jumps of the oscillation period and the intensity-velocity phase difference in both umbra-penumbra and penumbra-superpenumbra boundaries reflecting a drastic change of physical and/or magnetic conditions. Furthermore, the phase analysis shows a delay of the intensity response to the velocity variations in accordance to the physics of the observed sawtooth velocity behavior. Our phase analysis also suggests that most of the UFs oscillate incoherently, while the calmest umbral area seems to be associated with velocity spreading from neighboring UFs.

The results do not permit us to draw concrete conclusions on the association of UFs and RP waves and whether the latter are a visual pattern created by a common source with UFs or a trans-sunspot wave driven by UFs. However, the presented analysis provides further important constraints for future models of sunspot oscillations and RP waves.

Acknowledgements. KT and GT acknowledge financial support by the organizers of the meeting.

References

Alissandrakis, C.E., Georgakilas, A.A., & Dialetis, D. 1992, Solar Phys., 138, 93
Beckers, J.M., & Tallant, P.E. 1969, Solar Phys., 7, 351
Beckers, J.M., & Schultz, R.B. 1972, Solar Phys., 27, 61
Bhatnagar, A., Livingston, W.C., & Harvey, J.W. 1972, Solar Phys., 27, 80
Bogdan, T.J. & Judge, P.G. 2006, Phil.Trans.R.Soc. A, 364, 313
Brynildsen, N., Maltby, P., Leifsen, T., Kjeldseth-Moe, O., & Wilhelm, K. 1999, Solar Phys., 191, 129
Christopoulou, E.B., Georgakilas, A.A., & Koutchmy, S. 2000, A&A, 354, 305
Christopoulou, E.B., Skodras, A., Georgakilas, A.A., & Koutchmy, S. 2003, ApJ, 591, 416
Giovanelli, R.G. 1972, Solar Phys., 27, 71
Kneer, F., Mattig, W., & Uexküll, M.v. 1981, A&A, 102, 147
Lites, B.W. 1986, ApJ, 301, 992
Lites, B.W., 1992, in NATO ASIC Proc. 375, Sunspots: Theory and Observations, ed. J.H. Thomas, & N.O. Weiss, Kluwer Academic, Dordrecht, 261
Mein, P. 1991, A&A, 248, 669
Mein, P. 2002, A&A, 381, 271
Rouppe van der Voort, L.H.M., Rutten, R.J., Sütterlin, P., Sloover, P.J., & Krijger, J.M. 2003, A&A, 403, 277
Torrence, C., & Compo, G.P. 1998, Bull. Amer. Meteor. Soc., 79, 61

Tsiropoula, G., Alissandrakis, C.E., & Dialetis, D., & Mein, P. 1996, Solar Phys., 167, 79
Tsiropoula, G., Alissandrakis, C.E., & Mein, P. 2000, A&A, 355, 375
Tziotziou, K., Tsiropoula, G., & Mein, P. 2002, A&A, 381, 279
Tziotziou, K., Tsiropoula, G., & Sütterlin, P. 2005, A&A, 444, 265
Uexküll, M.v., Kneer, F., & Mattig, W. 1983, A&A, 123, 263
Zirin, H., & Stein, A. 1972, ApJ, 178, L85